PHOMS: an OCT marker of axoplasmic stasis in the optic nerve head

J. Alexander Fraser, MD[1], **Patrick A. Sibony, MD**[2], **Axel Petzold, MD, PhD**[3], **Caroline Thaung, MB, ChB, DPhil**[4], **Steffen Hamann, MD, PhD**[5], **ODDS Consortium**[6]

[1]Department of Clinical Neurological Sciences and Department of Ophthalmology, Western University, London, Ontario, Canada

[2]Department of Ophthalmology, State University of New York at Stony Brook, Stony Brook, NY, United States

[3]Moorfields Eye Hospital, London, UK; Department of Neurology, Amsterdam Neuroscience, VUmc MS Center Amsterdam and Dutch Expertise Centre for Neuro-ophthalmology, VU University Medical Centre, Amsterdam, The Netherlands; Institute of Neurology, University College London, London UK

[4]Department of Eye Pathology, UCL Institute of Ophthalmology, London, UK, and Moorfields Eye Hospital, London, UK

[5]Department of Ophthalmology, Rigshospitalet, University of Copenhagen, Copenhagen, Denmark

[6]See Appendix for Consortium members and affiliations

Abstract

Background: With the development and widespread adoption of spectral-domain OCT, peripapillary hyperreflective ovoid mass-like structures (PHOMS) have become a frequent OCT finding in neuro-ophthalmic practice. Though originally assumed to represent a form of buried optic disc drusen (ODD), PHOMS differ from ODD in many important ways. The histopathological underpinnings of PHOMS are now becoming more clearly understood.

Evidence Acquisition: Review of literature.

Results: PHOMS can be broadly classified as disc edema-associated PHOMS, ODD-associated PHOMS, or anomalous disc-associated PHOMS. PHOMS are seen in many conditions, including papilledema, nonarteritic anterior ischemic optic neuropathy, central retinal vein occlusion, acute

Corresponding Author: Dr. J. Alexander Fraser, Room B7-104, London Health Sciences Centre, University Hospital, 339 Windermere Road, London, ON, N6A 5A5, Canada, Phone: 519-663-3702, Alex.Fraser@lhsc.on.ca.

demyelinating optic neuritis, ODD, and tilted discs (myopic obliquely-inserted discs), and in many cases resolve along with the underlying condition. Histopathological study of these diverse entities reveals the common feature of a bulge of optic nerve fibers herniating centrifugally over Bruch's membrane opening (BMO) into the peripapillary space, correlating exactly with the location, shape, and space-occupying nature of PHOMS on OCT. Because of the radial symmetry of these herniating optic nerve fibers, PHOMS are best thought of as a complete or partial torus (*i.e.*, donut) in three dimensions.

Conclusions: PHOMS are a common but non-specific OCT marker of axoplasmic stasis in the optic nerve head. They are not themselves ODD or ODD precursors, though they can be seen in association with ODD as well as a wide spectrum of other conditions. They do not exclude papilledema and often accompany it. The circumferential extent and characteristic 3D toroidal nature of a PHOMS are best appreciated by scrolling through consecutive OCT images.

Keywords

PHOMS; EDI-OCT; optic nerve head; optic disc edema; optic disc drusen; optic nerve head drusen; tilted optic disc

Optical coherence tomography (OCT) has revolutionized retinal and optic nerve imaging. Until the development of spectral-domain OCT (SD-OCT), imaging of the peripapillary region and deep prelaminar optic nerve head was limited. These regions were obscured by shadowing from overlying structures and appeared as dark hyporeflective spaces on OCT, with no distinct internal features (1,2).

The development of SD-OCT in the mid-2000s (3,4), particularly the development of enhanced-depth imaging OCT (EDI-OCT) in 2008 (5), has improved both acquisition speed and depth of penetration. The lamina cribrosa, the inner edge of Bruch's membrane opening (BMO), and the peripapillary region immediately overlying the rim of BMO, can be visualized in exquisite and reproducible detail, and anatomical structures can be imaged *in vivo* with unprecedented ease and resolution (Figure 1A) (6,7,8).

One such structure, which has attracted attention and stirred some degree of controversy over the past few years, is the peripapillary hyperreflective ovoid mass-like structure, or "PHOMS" (pronounced "*fomms*"). In this review, we describe the morphological appearance of PHOMS on EDI-OCT, outline the spectrum of conditions in which PHOMS may be seen, discuss the histopathological counterparts of PHOMS and the role of axoplasmic stasis in their pathogenesis, and review the current confusion surrounding their resemblance to optic disc drusen (ODD). Finally, we highlight some unanswered questions regarding these structures and suggest possible new directions forward. Throughout this review, we use the acronym "PHOMS" as both a singular and plural form.

What is a PHOMS?

A typical PHOMS is depicted in Figure 1B. It is a common OCT accompaniment to many varieties of optic disc swelling, elevation, or tilt. Histopathological examinations and other lines of evidence indicate that a PHOMS is composed of herniated optic nerve fibers bulging

centrifugally into the peripapillary region as a result of axoplasmic stasis, and we review this evidence below. For this reason, the discovery of a PHOMS on an OCT is no mere curiosity; as the outward manifestation of pathophysiological processes at the optic disc level, a PHOMS signifies deeper microscopic and ultrastructural changes within the optic nerve. An elucidation of the cause and significance of PHOMS can better inform our understanding of the diagnosis and management of various optic neuropathies. Each letter of the acronym "PHOMS" describes a cardinal feature of the entity:

Peripapillary

A PHOMS is *peripapillary* in location, situated just above Bruch's membrane at the lip of BMO and external to the optic disc itself. It may have circumferential extent, following the edge of the circular BMO in a complete or partial torus (*i.e.*, "donut") configuration that correlates ophthalmoscopically with a pale C-shaped peripapillary "halo" obscuring the disc margin (8,9,10,11).

Hyperreflective

A PHOMS is diffusely *hyperreflective*, indicative of OCT beam scattering, and implying an inhomogeneous optical density throughout. This suggests a fine internal substructure, and new evidence is emerging that PHOMS contain their own microvasculature (8,10,11,12).

Ovoid

A PHOMS appears *ovoid* in shape on a typical B-scan (cross-sectional) OCT image. There is seldom any lobulation or complexity to this morphology, regardless of the underlying optic nerve pathology accompanying the PHOMS. Although its oval cross-sectional appearance may initially suggest an ellipsoid-like "lump" underlying the peripapillary retina, analogous to an isolated ODD, a PHOMS in three dimensions is better thought of as a partial torus than a discrete lump – more inner-tube than basketball (Figure 2) (13,14).

Mass-like Structure

A PHOMS is a *mass-like structure*, occupying space in the peripapillary region, often deflecting two or more of the overlying retinal layers anteriorly and radially outwards. This produces a "ski slope"-like appearance to the neighboring retinal architecture (6,15), which other authors have likened to a "boot shape" (16) or a "bend" (9). The degree of deflection of the overlying retinal layers depends significantly upon the distance of the OCT slice plane from the center of the optic disc (Figure 3).

Differentiation of PHOMS from mimics

These four cardinal features of a PHOMS, described above, combined with an appreciation of the structure's three-dimensional morphology (Supplemental Video), can be used to differentiate it from similar ovoid structures in the optic disc and peripapillary regions – retinal blood vessels and ODD (Figure 4). In this way, PHOMS are recognized with a high level of accuracy by different observers (interrater kappa 0.811–0.951) (15,17).

The EDI-OCT appearance of blood vessels is distinct from that of a PHOMS (Figure 4B). While blood vessels appear ovoid when imaged in cross-section and can have

a hyperreflective interior similar to a PHOMS, blood vessels have a sharply-defined hyperreflective anterior and posterior border, cast a long shadow over deeper structures, and appear in the inner, superficial layers of the optic disc and not the peripapillary region immediately overlying Bruch's membrane where PHOMS are found (6,18).

The appearance of an ODD is likewise distinct from that of a PHOMS (Figure 4C). An isolated ODD appears as discrete ellipsoid "lump" without cylindrical extent (like a blood vessel) or toroidal extent (like a PHOMS) on consecutive OCT slices. An ODD has a *hypo*reflective core and hyperreflective margins and, unlike PHOMS, is found within the optic nerve head. Its cross-sectional shape may be simple and ovoid or complex and multilobulated, particularly when it forms conglomerations with other ODD. Occasionally, especially in longstanding cases with very large ODD, smaller ODD can be seen within the interior of the PHOMS, like raisins in a bagel.

The spectrum of conditions in which PHOMS are seen

PHOMS were first observed in the early SD-OCT era, during studies of optic disc swelling (16) and pediatric tilted disc syndrome, in which they were described as "dome-like hyperreflective structures" (9). They have subsequently been observed in numerous contexts (Figure 5), including in papilledema (10,17,19), in ODD (6,10,17,20,21), in non-arteritic anterior ischemic optic neuropathy (NA-AION) (10,22,23), in central retinal vein occlusion (CRVO) (10), in optic neuritis (10,17), and in myopic/tilted optic discs (9,10,24). Given this wide spectrum of conditions, one helpful way to categorize PHOMS is by etiology: 1) Disc edema-associated PHOMS; 2) ODD-associated PHOMS; and 3) anomalous disc-associated PHOMS (25).

Indeed, PHOMS are common in these conditions. Among young patients with NA-AION, PHOMS were seen with a prevalence of 28% of 36 eyes without any other concomitant optic nerve pathology (such as ODD) (23). Among 227 patients with MS, PHOMS were found prospectively in 10% of eyes affected by optic neuritis and in 0% of 62 healthy controls (17). A retrospective component of this study examined PHOMS in 267 patients with other conditions and revealed a PHOMS prevalence of 62% in idiopathic intracranial hypertension (IIH), 47% in ODD, 44% in anomalous optic discs, and 19% in isolated non-MS optic neuritis (17).

Histopathological correlates of PHOMS

Because PHOMS are so prevalent in patients with IIH, it is useful to consider the histopathology and pathogenesis of papilledema as a model for understanding how PHOMS may arise in other diverse conditions (Figure 6, Figure 7).

Papilledema

Histopathological studies of the optic nerve head in papilledema have shown distended and vacuolated optic nerve axons anterior to the lamina cribrosa, particularly in the peripapillary part of the nerve (26,27). These optic nerve fibers bulge laterally over the rim of BMO (Figure 6C, Figure 7A), often folding over themselves into an S-shape and displacing

the peripapillary retinal layers laterally and upwards, while the retinal pigment epithelium and Bruch's membrane remain undistorted (Figure 6D) (26,27,28,29). The location and morphology of this bulge of herniated nerve fibers on histopathology correspond exactly with the location and morphology of disc edema-associated PHOMS as detected on OCT (10). Numerous small dilated venules and capillaries are evident within the optic nerve tissue and are most numerous just inside these laterally bulging nerve fibers (27). Interstitial fluid, extravasated from these vessels, further increases the turgid buckling of optic nerve fibers into the peripapillary space adjacent to BMO (26,28). Radioactive isotope studies in primate models of papilledema demonstrate stasis of axoplasmic transport, with a chokepoint at the lamina cribrosa (26). Electron microscopy methods, too, confirm axoplasmic stasis, with disrupted neurofilament proteins and an accumulation of giant mitochondria inside the distended prelaminar axons (Figure 8) (26). As papilledema resolves, clinically, and as centrifugally herniating nerve fibers recede back into the scleral canal, it is often observed that PHOMS regress too (Figure 5A,B) (10).

Optic disc drusen

The histopathology of the optic nerve head in ODD shares several important features with the histopathology in papilledema. While interstitial edema is largely absent in ODD because intracranial pressure is normal, axoplasmic stasis can nonetheless arise, in part due to mechanical compression of nerve fibers by the dense, rock-like, calcified ODD in the prelaminar optic nerve (Figure 7B) (30,31,32). As with papilledema, distended and vacuolated axons are present, typically in the tissue anterior to the ODD, with increased mitochondria suggestive of impaired axonal transport. Electron microscopy of these distended fibers reveals distressed axolemma and mitochondria with embedded needles of crystalline calcium (31). Neighboring small venules, too, may be compressed by ODD, causing upstream vascular congestion, though rarely frank edema. Consequently, a profusion of dilated small venules and capillaries may be seen in the vicinity of ODD (31). The typically narrow scleral canals of young patients with ODD may further aggravate this congestion (33).

When such axoplasmic stasis ensues in the setting of ODD, engorged optic nerve fibers bulge over the rim of BMO to form a lateral S-shaped bulge – the histopathological correlate of ODD-associated PHOMS (31,32). When ODD are large and multiple, the collective distention of axons causes a visible elevation of the disc (optic nerve "pseudoedema"). This concurrence of ODD and peripapillary nerve fiber bulging is not rare – in one retrospective study of 31 eyes with ODD (collected from a total of 1713 enucleated eyes), 5 eyes had localized peripapillary axonal bulging (32). The histological difference between ODD and peripapillary nerve fiber bulging remains stark, however, and it is abundantly clear that these bulges are neural tissue – and not anything reminiscent of ODD, "ODD precursors", or "noncalcified ODD". They even stain positive for nerve fibers using S100 immunostaining (10). ODD, by contrast, appear histologically as rounded, acellular, hyaline deposits, uniform in density with no significant internal substructure (18,30,31). They are found exclusively anterior to the lamina cribrosa and are always calcified (30,31,32).

Other entities

The pathogenic mechanisms that produce peripapillary nerve fiber bulges in papilledema and in ODD – namely, axoplasmic stasis with or without interstitial edema – are seen in other causes of optic disc edema. It is not a surprise, therefore, to see disc edema-associated PHOMS in several other conditions. For example, in the histopathology of both NA-AION (Figure 7C) (34) and CRVO (Figure 7D) (35), swollen vacuolated optic nerve axons are seen to bulge over the edge of BMO and crowd the retina laterally.

An identical picture of lateral S-shaped bulging of swollen, distressed, mitochondria-laden prelaminar optic nerve fibers can even be produced experimentally in monkeys by ligating a portion of the immediately retrobulbar optic nerve (but avoiding the neighboring vessels) (Figure 7E). In this animal model, radiotracer studies demonstrate that the characteristic histopathological changes are primarily the result of axoplasmic stasis and not interstitial fluid collection (36). A similar phenomenon can occur in the optic nerve heads of humans undergoing surgical enucleation. Clamping of the retrobulbar optic nerve during the surgery results in abrupt axoplasmic stasis and vascular occlusion, resulting in a herniation (or "toothpasting") of optic nerve fibers centrifugally over BMO (29). Ocular pathologists must be careful to recognize this optic nerve head abnormality as an artefact of surgery and not necessarily a feature of the underlying ocular disease.

Human histopathological studies of the optic nerve head in acute demyelinating optic neuritis are lacking – presumably due to the rarity of enucleation or autopsy during the acute phase of inflammation. However, in one study using the juvenile guinea pig model of experimental autoimmune optic neuritis, the typical histopathological findings of optic neuritis included a mononuclear cell infiltration posterior to the lamina cribrosa accompanied by myelin loss and inflammatory perivascular cuffs (37). Anterior to the lamina cribrosa, this inflammation was not found, but optic disc edema was evident with markedly swollen axons displacing the peripapillary retina laterally in an S-shaped bulge (Figure 7F) (37). Electron microscopy of these notably distended axons revealed an accumulation of degenerating mitochondria and a disorganized scaffold of neurofilament proteins – the hallmarks of axoplasmic stasis (38). While perilaminar inflammatory congestion is one plausible mechanism for axoplasmic stasis in optic neuritis, emerging literature in humans with MS suggests that impairments in the ocular glymphatic system could also impede axonal transport and may contribute to these histomorphological distortions underlying PHOMS (17,27,39,40).

Tilted optic discs are a common optic nerve head variant in the general population and do not cause acute injury to the optic nerve; however, like discs with ODD, their abnormal morphology predisposes to chronic focal axoplasmic stasis. In the nasal prelaminar optic nerve there are two main locations of nerve fiber bundle impingement: first, Bruch's membrane protrudes towards the optic nerve along its upper extent, forcing the optic nerve fibers to bend sharply as they descend into the scleral canal (9,41); second, the nasal dragging of the lamina cribrosa relative to BMO and the slow stretching of the sclera and lamina cribrosa – thought to underlie the pathogenesis of optic disc tilt – may cause focal stress on optic nerve axons as they pass through pores of the lamina cribrosa, particularly in the fibers subserving the nasal optic disc (9,42,43). Some degree of chronic axoplasmic

stasis ensues, with the familiar S-shaped peripapillary bulge of enlarged, vacuolated nerve fibers forming nasally (Figure 7G) (44). Nasal pseudopapilledema and optic disc elevation occur, evident ophthalmoscopically and on *en face* OCT as a characteristic C-shaped halo. Cross-sectional EDI-OCT through this halo reveals an anomalous disc-associated PHOMS (Figure 5H) (9,11,45,46). Given their high prevalence, tilted optic discs are a major cause of pseudopapilledema in clinical practice and, consequently, a commonly encountered cause of PHOMS (9,47). Over time, these congested axons can atrophy, and temporal visual field defects may emerge (9,48). In a recent study comparing children with PHOMS to children without PHOMS, PHOMS were significantly associated with myopia, and optic disc tilt appeared to be the unifying explanation (24).

Commonalities

The histopathology of each of the above entities has shown the common feature of a peripapillary S-shaped bulge of nerve fibers, whose axons appear distended and vacuolated; these fibers are constipated with large degenerating mitochondria that are unable to move distally because of axoplasmic stasis (Figure 8). Small dilated veins and capillaries permeate the bulge. In the case of papilledema, interstitial edema may further contribute to the tumescence of prelaminar tissue and the centrifugal expansion of optic nerve fibers. Irrespective of the underlying cause, this bulge herniates in a stereotyped fashion laterally between Bruch's membrane and the inner layers of the retina in an S-shape, the bottom fold of the S forming an ovoid mass-like structure that displaces the overlying retina centrifugally and anteriorly. In the interior of the bulge, the myriad optical interfaces between nerve fibers, vacuoles, capillaries, and interstitial fluid compartments produce multiple internal reflections and refractions, which scatter light and render the structure diffusely hyperreflective on OCT, appearing as a PHOMS. Not surprisingly, high-resolution OCT angiography has recently confirmed the presence of dense networks of small vessels within PHOMS of various different etiologies (11).

Drusen Confusion

A PHOMS has a superficial resemblance to an ODD on cross-sectional OCT B-scan imaging: a PHOMS appears approximately the same size as a moderate-sized ODD, and, like an ODD, a PHOMS occupies space and appears ovoid in cross-section (Figures 4A,C). In the early days of SD-OCT and EDI-OCT, as the prelaminar optic nerve was being studied *in vivo* for the first time, it was sometimes believed that PHOMS *were themselves* ODD (16,20,49,50); however, our understanding of the distinction between PHOMS and ODD has evolved over the past 5–10 years, especially now that PHOMS have been observed ubiquitously in many other conditions besides ODD (Figure 5) (9,10,11,17,18,22,23), now that PHOMS have been reported to disappear as disc edema resolves (Figures 5A,B,F,G) (10), and now that PHOMS have been observed to form a complete torus 360º around the optic disc (an implausible shape for an ODD) (14).

In cross-sectional images of the optic nerve head (Figure 3A, C, E-H), displacement of the inner nuclear layer (INL) defines a hyporeflective boundary between a PHOMS and the retinal nerve fiber layer (RNFL) (yellow arrows in Figure 3C, F, G). Some have claimed

that this border completely surrounds the PHOMS, forming an isolated non-neural mass, presumed to be an ODD (45). However, serial sagittal cross sections of PHOMS refute this, showing that there is no border between PHOMS and the RNFL in the central regions of the optic nerve head (Figure 3H), where distended axons double back around the INL to form the RNFL. The continuity between distended axons in a PHOMS and the RNFL can be demonstrated in patients with papilledema (Figure 3), as well as in patients with ODD and tilted discs.

Unlike ODD, PHOMS are not detectable with other imaging modalities such as orbital ultrasound, fundus autofluorescence imaging, or CT orbits (6,12,51,52). It has been suggested that PHOMS may therefore be a form of noncalcified ODD (45,53). While allusions to noncalcified ODD can be found in the literature, there is no actual histological basis for "noncalcified ODD": among 48 eyes with true ODD, painstakingly extracted from a broad collection of more than three thousand eyes examined at autopsy (30) or after enucleation (32), not a single instance of an accompanying noncalcified ODD was found. Small hyperreflective dots have recently been documented inside PHOMS on OCT, and proposed to represent microcalcifications and possible "ODD precursors" (46). This is highly speculative, however, as such dots are nonspecific, can be found throughout the retina, and are seen in PHOMS of all etiologies, not just ODD-associated PHOMS (54,55,56,57). Furthermore, they seem to resolve when the PHOMS does (Figures 5A,B,F,G).

The claim that PHOMS are a type of ODD has been refuted before (6,12,19,25), and key differences between the two entities are summarized in Table 1. Centrifugally bulging nerve fibers easily explain PHOMS in all clinical settings. Although some degree of confusion still persists in the literature (45,58,59), the evidence is overwhelming now that PHOMS are not ODD.

Future directions

With the increasingly widespread availability of EDI-OCT and SS-OCT technology, offering deeper penetration into the prelaminar optic nerve head at higher resolutions than ever before, neuro-ophthalmologists are in the vanguard for detecting, following, and studying PHOMS. Many unanswered questions about these fascinating structures remain, including: Does PHOMS size correlate with other measurements of optic disc edema (*e.g.*, Frisén grade in papilledema)? Can early detection of PHOMS on OCT predict papilledema recurrence in IIH? Can quantitative measurements of PHOMS (surface area, volume) be used to predict visual outcomes in neuro-ophthalmic disease? Does the size or location of a PHOMS predict visual field loss in ODD? In tilted disc syndrome, does the presence or size of a nasal PHOMS correlate directly with temporal visual field depression? What role does the translaminar pressure gradient play in the evolution of PHOMS? Though PHOMS are certainly a marker of axoplasmic stasis in many common neuro-ophthalmic conditions, are they strictly an epiphenomenon, or do they carry their own independent risks to vision (e.g., from kinking of nerve fibers around the S-shaped bend or from shear stresses on the intrinsic optic nerve microvasculature)? The study of PHOMS is in its early stages, and a fuller understanding of this novel OCT marker of axoplasmic stasis awaits.

Supplementary Material

Refer to Web version on PubMed Central for supplementary material.

Appendix

Members of the Optic Disc Drusen Studies (ODDS) Consortium are:

Aghsaei Fard, Masoud (Tehran University of Medical Science, Tehran, Iran)

Beres, Shannon (Stanford University Medical Centre, Palo Alto, California, USA)

Biousse, Valérie (Emory University School of Medicine, Atlanta, USA)

Bursztyn, Lulu (Ivey Eye Institute, Western University, London, Ontario, Canada)

Crum, Alison (University of Utah, Salt Lake City, Utah, USA)

Digre, Kathleen B. (University of Utah, Salt Lake City, Utah, USA)

Fraser, J. Alexander (Western University, London, Ontario, Canada)

Fraser, Clare L. (Save Sight Institute, University of Sydney, Australia)

Gale, Jesse (Wellington, New Zealand)

Hamann, Steffen (Rigshospitalet, University of Copenhagen, Glostrup, Denmark)

Huna-Baron, Ruth (Sheba Medical Center, Tel Hashomer, Israel)

Katz, Bradley (University of Utah, Salt Lake City, Utah, USA)

Lawlor, Mitchell (Sydney Eye Hospital, University of Sydney, Australia)

Liao, Yaping Joyce (Stanford University Medical Centre, Palo Alto, California, USA)

Malmqvist, Lasse (Rigshospitalet, University of Copenhagen, Glostrup, Denmark)

Maloca, Peter M. (Institute of Molecular and Clinical Ophthalmology (IOB), Basel, Switzerland)

Moss, Heather E. (Stanford University Medical Centre, Palo Alto, California, USA)

Newman, Nancy J. (Emory University School of Medicine, Atlanta, USA)

Peragallo, Jason H. (Emory University School of Medicine, Atlanta, USA)

Petzold, Axel (Moorfields Eye Hospital, London, UK)

Rasool, Nailyn (University of California San Francisco, California, USA)

Rodriguez, Amadeo (McMaster University, Hamilton, Ontario, Canada)

Rothenbuehler, Simon P. (University Hospital Basel, Switzerland)

Rougier, Marie-Bénédicte (Centre Hospitalier Universitaire de Bordeaux, France)

Sibony, Patrick A. (Department of Ophthalmology, State University of New York at Stony Brook, New York, USA

Subramanian, Prem S. (University of Colorado School of Medicine, Denver, Colorado, USA)

Warner, Judith E. A. (University of Utah, Salt Lake City, Utah, USA)

Wegener, Marianne (Rigshospitalet, University of Copenhagen, Glostrup, Denmark)

Wong, Sui H. (Moorfields Eye Hospital, London, UK)

REFERENCES

1. Johnson LN, Diehl ML, Hamm CW, Sommerville DN, Petroski GF. Differentiating optic disc edema from optic nerve head drusen on optical coherence tomography. Arch Ophthalmol 2009; 127:45–49. [PubMed: 19139337]

2. Flores-Rodriguez P, Gili P, Martin-Rios MD. Sensitivity and specificity of time-domain and spectral-domain optical coherence tomography in differentiating optic nerve head drusen and optic disc oedema. Ophthalmic Physiol Opt 2012; 32:213–221. [PubMed: 22428958]

3. Wojtkowski M, Bajraszewski T, Gorczynska I, Targowski P, Kowalczyk A, Wasilewski W, Radzewicz C. Ophthalmic imaging by spectral optical coherence tomography. Am J Ophthalmol 2004; 138:412–419. [PubMed: 15364223]

4. Nassif N, Cense B, Park BH, Yun SH, Chen TC, Bouma BE, Tearney GJ, de Boer JF. In vivo human retinal imaging by ultrahigh-speed spectral domain optical coherence tomography. Opt Lett 2004; 29:480–482. [PubMed: 15005199]

5. Spaide RF, Koizumi H, Pozonni MC. Enhanced depth imaging spectral-domain optic coherence tomography. Am J Ophthalmol 2008; 146:496–500. [PubMed: 18639219]

6. Malmqvist L, Bursztyn L, Costello F, Digre K, Fraser JA, Fraser C, Katz B, Lawlor M, Petzold A, Sibony P, Warner J, Wegener M, Wong S, Hamann S. The Optic Disc Drusen Studies consortium recommendations for diagnosis of optic disc drusen using optical coherence tomography. J Neuroophthalmol 2018; 38:299–307. [PubMed: 29095768]

7. Tatar IT, Solmaz B, Erdem ZG, Pasaoglu I, Dermircan A, Tulu Aygyn B, Ozkaya A. Morphological assessment of lamina cribrosa in idiopathic intracranial hypertension. Ind J Ophthalmol 2020; 68:164–167.

8. Lopes FS, Matsubara I, Almeida I, Dorairaj SK, Vessani RM, Paranhos A Jr, Prata TS. BMC Ophthalmol 2019; 19:52. [PubMed: 30770751]

9. Pichi F, Romano S, Villani E, Lembo A, Gilardoni F, Morara M, Ciardella AP, Ohno-Matsui K, Nucci P. Spectral-domain optic coherence tomography findings in pediatric tilted disc syndrome. Graefes Arch Clin Exp Ophthalmol 2014. 252:1661–1667. [PubMed: 25038908]

10. Malmqvist L, Sibony PA, Fraser CL, Wegener M, Heegaard S, Skougaard M, Hamann S, Optic Disc Drusen Studies Consortium. Peripapillary ovoid hyperreflectivity in optic disc edema and pseudopapilledema. Ophthalmology 2018; 125:1662–1664. [PubMed: 29891127]

11. Borrelli E, Barboni P, Battista M, Sacconi R, Querques L, Cascavilla ML, Bandello F, Querques G. Peripapillary hyperreflective ovoid mass-like structures (PHOMS): OCTA may reveal new findings. Eye (Lond) 2020 Apr 28. doi: 10.1038/s41433-020-0890-4. Online ahead of print.

12. Malmqvist L, Bursztyn L, Costello F, Digre K, Fraser JA, Fraser C, Katz B, Lawlor M, Petzold A, Sibony P, Warner J, Wegener M, Wong S, Hamann S. Peripapillary hyperreflective ovoid

mass-like structures: is it optic disc drusen or not?. Response. J Neuroophthalmol 2018; 38:568–570. [PubMed: 29901493]

13. Moroni L. The toric sections: a simple introduction. arXiv:1708.00802 [math.HO] [Preprint] 2017. Available from: https://arxiv.org/pdf/1708.00803.

14. Fraser JA, Hamann S. A 360-degree peripapillary hyperreflective ovoid mass-like structure. Can J Ophthalmol 2020 (in press)

15. Petzold A, Biousse V, Bursztyn LLCD, Costello F, Crum AW, Digre KB, Fraser CL, Fraser JA, Katz BJ, Jurkute N, Newman NJ, Nowomiejska K, Frederiksen JL, Mitchell L, Liskova P, Lorenz B, Malmqvist L, Pergallo J, Sibony PA, Subramanian PS, Rejdak R, Touitou V, Warner JEA, Wegener M, Wong SH, Yu-Wai-Man P, Hamann S, on behalf of the ODDS Consortium and ERN-EYE. Multirater validation of peripapillary hyperreflective ovoid mass-like structures (PHOMS). Neuroophthalmol 2020 (in press)

16. Lee KM, Woo SJ, Hwang JM. Differentiation of optic nerve head drusen and optic disc edema with spectral-domain optical coherence tomography. Ophthalmology 2011; 118:971–977. [PubMed: 21211843]

17. Petzold A, Coric D, Balk LJ, Hamann S, Uitdehaag BMJ, Denniston AK, Keane PA, Crabb DP. Longitudinal development of PHOMS suggest a novel pathological pathway. Ann Neurol 2020 May 19. doi: 10.1002/ana.25782. Online ahead of print.

18. Fraser JA, Bursztyn LLCD. Optical coherence tomography in optic disc drusen. Ann Eye Sci 2020. 5;5.

19. Malmqvist L, Fraser C, Fraser JA, Lawlor M, Hamann S. RE: Traber et al: enhanced depth imaging optical coherence tomography of optic nerve head drusen: a comparison of cases with and without visual field loss. Ophthalmology 2017; 124: e55–e56. [PubMed: 28528842]

20. Traber GL, Weber KP, Sabah M, Keane PA, Plant GT. Enhanced depth imaging optical coherence tomography of optic nerve head drusen: a comparison of cases with and without visual field loss. Ophthalmology 2016; 124:66–73. [PubMed: 27817914]

21. Teixeira FJ, Marques RE, Man SS, Couceiro R, Pinto F. Optic disc drusen in children: morphological features using EDI-OCT. Eye (Lond) 2019 Nov 19. doi: 10.1038/s41433-019-0694-6. Online ahead of print.

22. Fraser JA, Ruelokke LL, Malmqvist L, Hamann S. Prevalence of optic disc drusen in young patients with nonarteritic anterior ischemic optic neuropathy: a 10-year retrospective study. J Neuroophthalmol 2020 Apr 30. doi: 10.1097/WNO.0000000000000974. Online ahead of print.

23. Hamann S, Malmqvist L, Wegener M, Biousse V, Bursztyn L, Citirak G, Costello F, Crum AV, Digre K, Fard MA, Fraser JA, Huna-Baron R, Katz B, Lawlor M,Newman NJ, Peragallo JH, Petzold A, Sibony PA, Subramanian PS, Warner JE, Wong SH, Fraser CL, Optic Disc Drusen Studies Consortium. Young adults with anterior ischemic optic neuropathy: a multicenter optic disc drusen study. Am J Ophthalmol 2020 Apr 13: S0002-9394(20)30164-1. doi: 10.1016/j.ajo.2020.03.052. Online ahead of print.

24. Lyu IJ, Park KA, Oh SY. Association between myopia and peripapillary hyperreflective ovoid mass-like structures in children. Sci Rep 2020; 10:2238. doi: 10.1038/s41598-020-58829-3. [PubMed: 32041993]

25. Sibony PA, Biousse V, Bursztyn L, Costello F, Digre K, Fraser JA, Fraser C, Huna-Baron R, Katz B, Lawlor M, Malmqvist L, Newman NJ, Peragallo J, Petzold A, Subramanian PS, Warner JEA, Wegener M, Wong S, Hamann S; ODDS Consortium. Comment on: Morphological features of buried optic disc drusen on en face optical coherence tomography and optical coherence tomography angiography. Am J Ophthalmol 2020 Jun 13: S0002-9394(20)30168-9. Online ahead of print.

26. Hayreh SS. Pathogenesis of optic disc edema in raised intracranial pressure. Prog Retin Eye Res 2016; 50: 108–144. [PubMed: 26453995]

27. Paton L, Holmes G. The pathology of papilledema: a historical study of sixty eyes. Brain 1911; 33: 389–432.

28. Sommers IG. Papilledema. In: Sommers IG. Histology and Histopathology of the Eye and its Adnexa London: Butterworth-Heinemann. 1949: 404–406

29. Proia AD, Cummings TJ. Eye and ocular adnexa. In: Mills SE. Histology for Pathologists, 5th ed. Philadelphia: Wolters-Kluwer. 2020: 350–4.

30. Friedman AH, Beckerman B, Gold DH, Walsh JB, Gartner S. Drusen of the optic disc. Surv Ophthalmol 1977; 21:373–90. [PubMed: 68551]

31. Tso MO. Pathology and pathogenesis of drusen of the optic nervehead. Ophthalmology 1981; 88:1066–80. [PubMed: 7335311]

32. Skougaard M, Heegaard S, Malmqvist L, Hamann S. Prevalence and histopathological signatures of optic disc drusen based on microscopy of 1713 enucleated eyes. Acta Ophthalmol 2020; 98:195–200. [PubMed: 31264343]

33. Malmqvist L, Li XQ, Eckmann CL, Skovgaard AM, Olsen EM, Larsen M, Munch IC, Hamann S. Optic disc drusen in children: the Copenhagen Child Cohort 2000 eye study. J Neuroophthalmol 2018; 38:140–146. [PubMed: 28841585]

34. Knox DL, Kerrison JB, Green WR. Histopathologic studies of ischemic optic neuropathy. Tr Am Ophth Soc 2000; 98:203–222. [PubMed: 11190024]

35. Green WR, Chan CC, Hutchins GM, Terry JM. Central retinal vein occlusion: a prospective histopathologic study of 29 eyes in 28 cases. Retina 1981; 1:27–55. [PubMed: 15633406]

36. Wirtschafter J. Optic nerve axons and acquired alterations in the appearance of the optic disc. Trans Am Ophthalmol Soc 1983; 81:1034–1091. [PubMed: 6203209]

37. Rao NA. Chronic experimental allergic optic neuritis. Invest Ophthalmol Vis Sci 1981; 20:159–172. [PubMed: 6161902]

38. Petzold A. Neurofilament phosphoforms: surrogate markers for axonal injury, degeneration and loss. J Neurol Sci 2005; 233:183–198. [PubMed: 15896809]

39. Petzold A. Retinal glymphatic system: an explanation for transient retinal layer volume changes? Brain 2016; 139:2816–2819. [PubMed: 29106485]

40. Denniston AK, Keane PA. Paravascular pathways in the eye: is there an ocular glymphatic system? Invest Ophthalmol Vis Sci 2015; 56:3955–3956. [PubMed: 26087361]

41. Enoch JM, Crawford JB, Howes EL, Choi SS, Ling D, Lee J, Nadadur M, Laverny K. Encroachment of the retina and choroid onto the nasal portion of the optic nerve head in high myopia: visual and anatomical manifestations. J Mod Opt 2009; 56: 2295–2308.

42. Kim TW, Kim M, Weinreb RN, Woo SJ, Park KH, Hwang JM. Optic disc change with incipient myopia of childhood. Ophthalmology 2012; 119:21–16. [PubMed: 21978594]

43. Lee KM, Choung HK, Kim M, Oh S, Kim SH. Positional change of optic nerve head vasculature during axial elongation as evidence of lamina cribrosa shifting: Boramae myopia cohort study report 2. Ophthalmology 2018; 125:1224–1233. [PubMed: 29544962]

44. Naumann GOH, Apple DJ. Malformations and Anomalies of the Eye. In: Naumann GOH, Apple DJ. Pathology of the Eye New York: Springer-Verlag. 1986: 78–79.

45. Kim MS, Lee KM, Hwang JM, Yang HK, Woo SJ. Morphological features of buried optic disc drusen on en fact optical coherence tomography and optical coherence tomography angiography. Am J Ophthalmol 2020. 213;125–133. [PubMed: 31987902]

46. Mezad-Koursh D, Klein A, Rosenblatt A, Teper Roth S, Neudorfer M, Loewenstein A, Iglicki M, Zur D. Peripapillary hyperreflective ovoid mass-like structures – a novel entity as frequent cause of pseudopapilloedema in children. Eye (Lond) 2020 Jul 2. Doi: 10.1038/s41433-020-1067-x. Online ahead of print.

47. Sibony PA, Kupersmith MJ, Kardon RH. OCT neuro-toolbox for the diagnosis and management of papilledema, optic disc edema, and pseudopapilledema. J Neuroophthalmol 2020. [In press]

48. Witmer MT, Margo CE, Drucker M. Tilted optic disks. Surv Ophthalmol 2010; 55:403–428. [PubMed: 20621322]

49. Kulkarni KM, Pasol J, Rosa PR, Lam BL. Differentiating mild papilledema and buried optic nerve head drusen using spectral domain optical coherence tomography. Ophthalmology 2014; 121:959–963. [PubMed: 24321144]

50. Bassi ST, Mohana KP. Optical coherence tomography in papilledema and pseudopapilledema with and without optic nerve head drusen. Indian J Ophthalmol 2014; 62:1146–1151. [PubMed: 25579359]

51. Costello F, Rothenbuehler SP, Sibony PA, Hamann S, for the Optic Disc Drusen Studies Consortium. Diagnosing optic disc drusen in the modern imaging era: a practical approach. Neuroophthalmol 2020. (In press)

52. Wang DD, Leong JCY, Gale J, Wells AP. Multimodal imaging of buried optic nerve head drusen. Eye (Lond) 2018. 32:1145–1156. [PubMed: 29379102]

53. Lee KM, Woo SJ, Hwang JM. Peripapillary hyperreflective ovoid mass-like structures: is it optic disc drusen or not? J Neuroophthalmol 2018; 38:566–574. [PubMed: 29595558]

54. Bolz M, Schmidt-Erfurth U, Deak G, Mylonas G, Kriechbaum K, Scholda C, Diabetic Retinopathy Research Group Vienna. Optical coherence tomographic hyperreflective foci: a morphologic sign of lipid extravasation in diabetic macular edema. Ophthalmology 2009; 116:914–20. [PubMed: 19410950]

55. Coscas G, De Benedetto U, Coscas F, Li Calzi CI, Vismara S, Roudot-Thoraval F, Bandello F, Souied E. Hyperreflective dots: a new spectral-domain optical coherence tomography entity for follow-up and prognosis in exudative age-related macular degeneration. Ophthalmologica 2013; 229:32–37. [PubMed: 23006969]

56. Saito M, Barbazetto IA, Spaide RF. Intravitreal cellular infiltrate imaged as punctate spots by spectral-domain optical coherence tomography in eyes with posterior segment inflammatory disease. Retina 2013; 33:559–65. [PubMed: 23042101]

57. Torm MEW, Belmouhand M, Munch IC, Larsen M, Rothenbuehler SP. Migration of an outer retinal element in a healthy child followed by longitudinal multimodal imaging. Am J Ophthalmol Case Rep 2020; 18:100637. [PubMed: 32154438]

58. Chang MY, Velez FG, Demer JL, Bonelli L, Quiros PA, Arnold AC, Sadun AA, Pineles SL. Accuracy of diagnostic imaging modalities for classifying pediatric eyes as papilledema versus pseudopapilledema. Ophthalmology 2017; 124:1839–1848. [PubMed: 28732589]

59. Jia X, Bao T, Wang S, Jiang T, Zhong Z, Zhang Y, Li Q, Zhu X. Diagnostic value of systematic imaging examination in embedded optic disc drusen in adolescents with mild visual impairment. J Ophthalmol 2020 Apr 3;2020:6973587. doi: 10.1155/2020/6973587. [PubMed: 32322411]
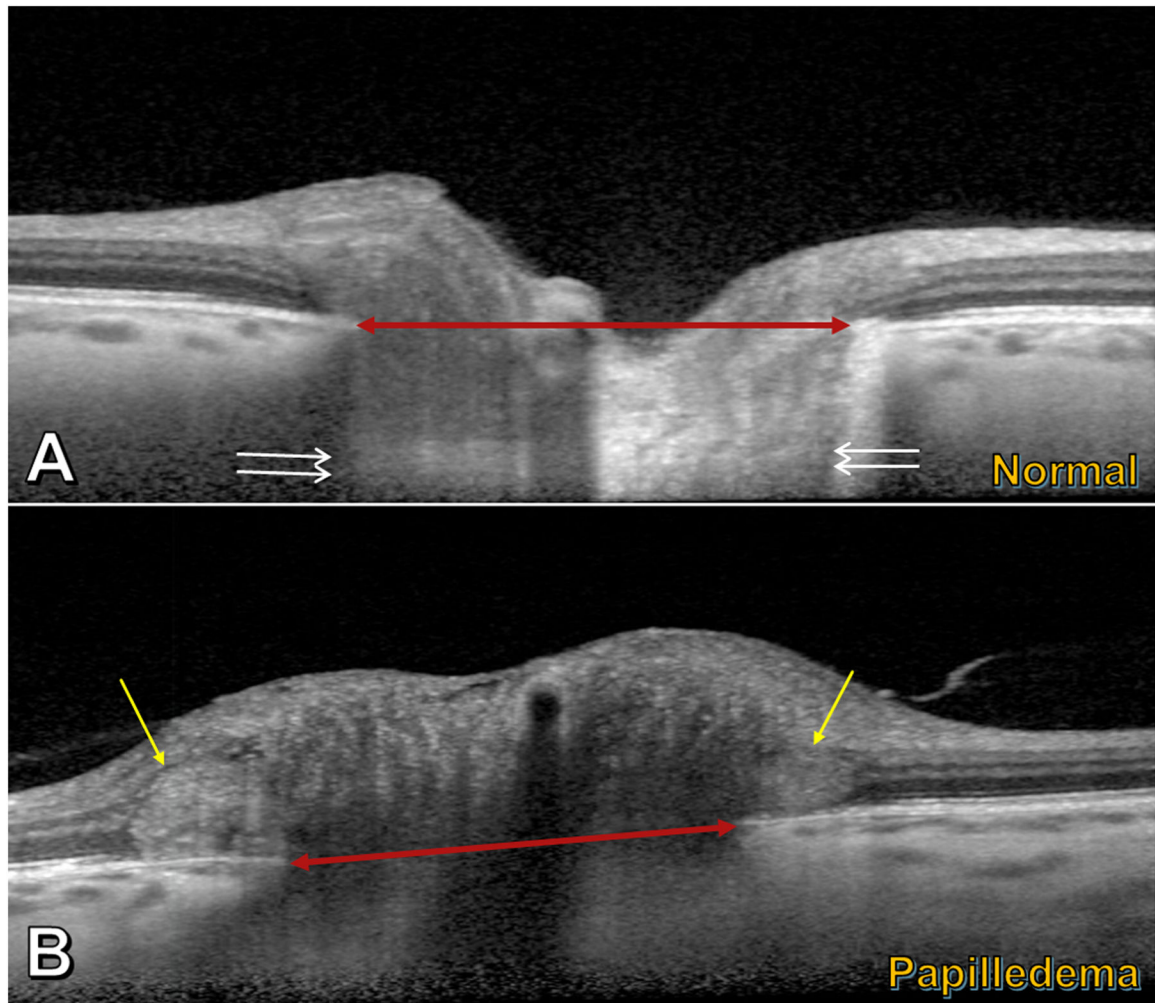
Figure 1 –.
Enhanced-depth imaging OCT transecting the optic nerve head. A) Normal eye: features include Bruch's membrane opening (BMO) (red double arrowhead) and lamina cribrosa (between pairs of white arrows). B) Papilledematous eye (in a patient with idiopathic intracranial hypertension): PHOMS (yellow arrows) are seen in the peripapillary region on either side of BMO (red double arrowhead), just above the Bruch's membrane/retinal pigment epithelium complex; the PHOMS are hyperreflective (light grey), stereotypically ovoid in shape, and deflect the retinal layers upwards and laterally.
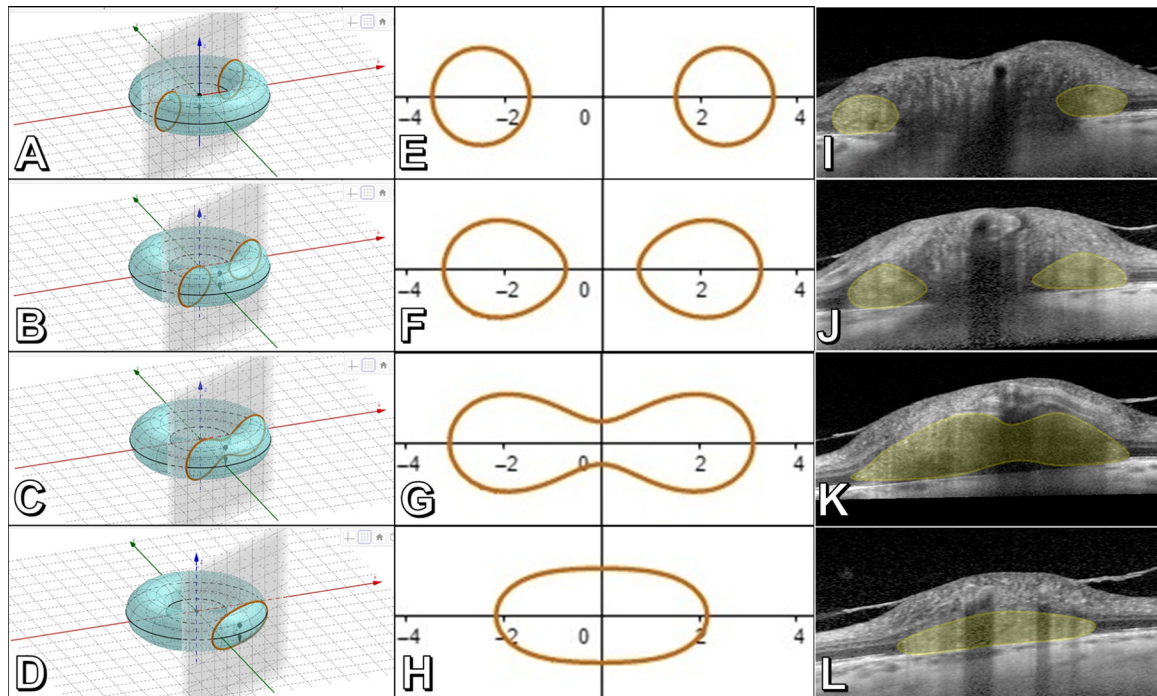
Figure 2 –.

The toroidal nature of a PHOMS. Panels A-D: An idealized torus (*i.e.*, donut) transected at different distances from the center by a plane perpendicular to the torus' central axis, representing B-scan OCT "slices" through a PHOMS. Panels E-H: Corresponding "toric sections" (known as "Cassini's ovals") arising from each idealized cut in A-D. Panels I-L: Real-world B-scan EDI-OCT slices though a papilledematous optic disc at the distances depicted in panels A-D, confirming the toroidal nature of a PHOMS (yellow shading). (Panels A-H created using the Geogebra applet at https://lucamoroni.it/simulations/intersection-torus-plane-simulation/ (13))
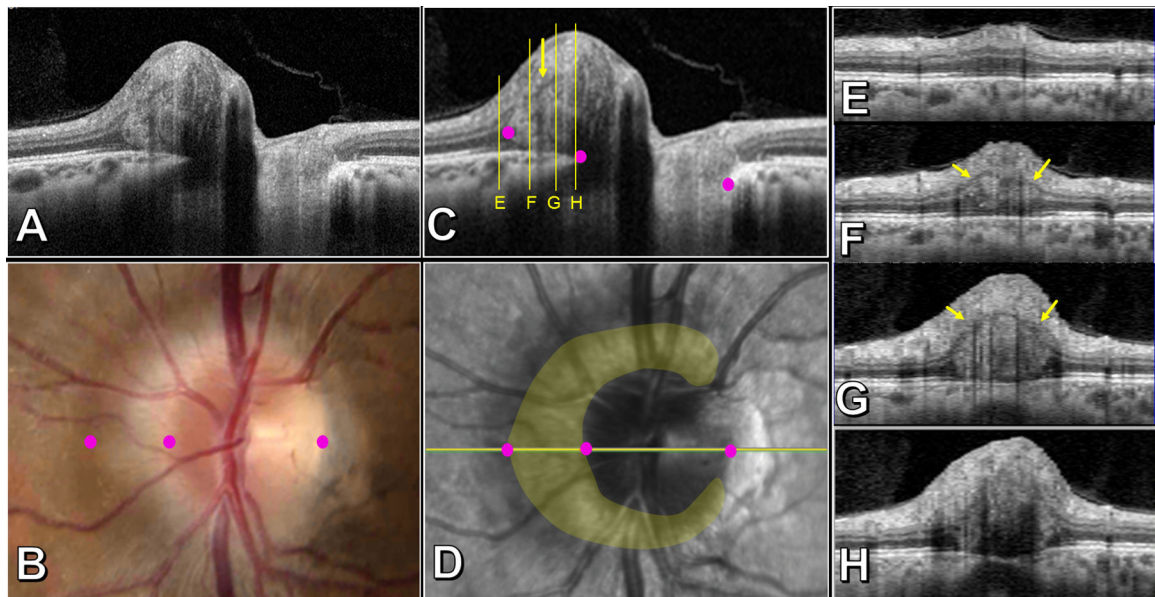
Figure 3 –.

Salient features of a PHOMS in a patient with papilledema, left eye. Transverse axial OCT (A and C), optic disc photo (B), confocal scanning laser ophthalmoscopic image (D), and sagittal cross-sectional OCTs through the nasal optic disc (E-H). The corresponding margins of the Bruch's membrane opening and nasal edge of the PHOMS are identified with magenta dots in images B, C, D. The yellow overlay in D shows that the PHOMS is a C-shaped partial torus that surrounds the disc nasally, superiorly, and inferiorly, sparing the temporal quadrant. The nasal bulge of the PHOMS abuts and splays the surrounding retina (E-H): the inner nuclear layer (INL) is displaced superiorly and appears as a fine hypodense line that forms the superior border of the PHOMS (small yellow arrows in C, F, G); panel E demonstrates widening of the outer nuclear layer just beyond the PHOMS' border. Panel H depicts the junction between PHOMS and RNFL where the INL is no longer visible. As the level of the image slice in E-H approaches the center of the disc, the deflection of overlying retinal layers, likened to a "ski slope" becomes steeper; tangential B-scans may therefore underestimate the true mass effect of the PHOMS on the overlying retinal layers.
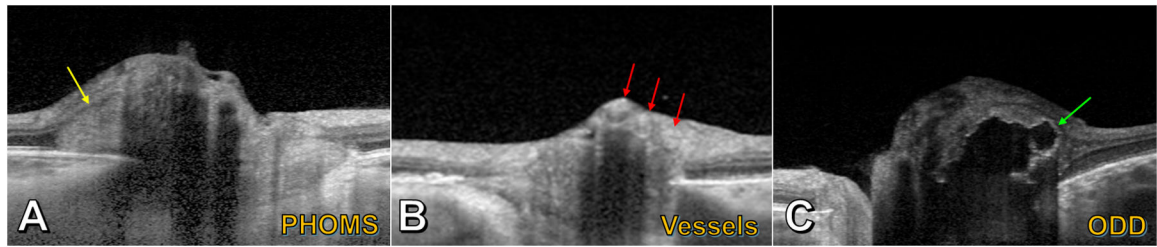
Figure 4 –.

Enhanced-depth imaging OCT of PHOMS and mimics. A) A PHOMS (yellow arrow) in the peripapillary region appears hyperreflective and deflects the retinal layers upwards and laterally; though the left part of the PHOMS appears ovoid, the right part of the PHOMS is obscured by an overlying shadow. B) Blood vessels (red arrows) appear as superficial circular structures casting long dark shadows; their tubular 3D structures are revealed by scrolling through consecutive OCT slices. C) A large lobulated optic disc drusen (ODD) (green arrow) is identifiable by its hyperreflective "shell" and hyporeflective core.
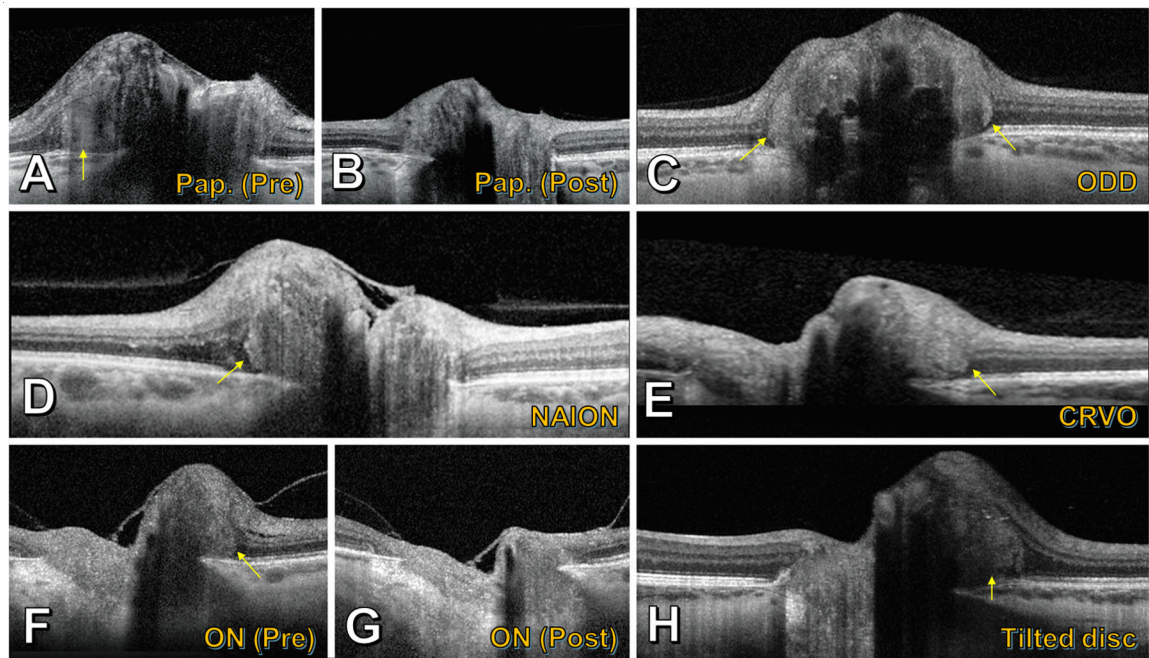
Figure 5 –.
Enhanced-depth imaging OCT depicting PHOMS (yellow arrows) in a spectrum of conditions. A) Patient with papilledema from idiopathic intracranial hypertension, who had B) significant reduction in the PHOMS after six months of weight loss and acetazolamide. C) Optic disc drusen. D) Acute nonarteritic anterior ischemic optic neuropathy. E) Acute central retinal vein occlusion. F) Patient with isolated acute demyelinating optic neuritis, who had G) significant reduction in the PHOMS following treatment with high-dose corticosteroids. H) Tilted optic disc syndrome.
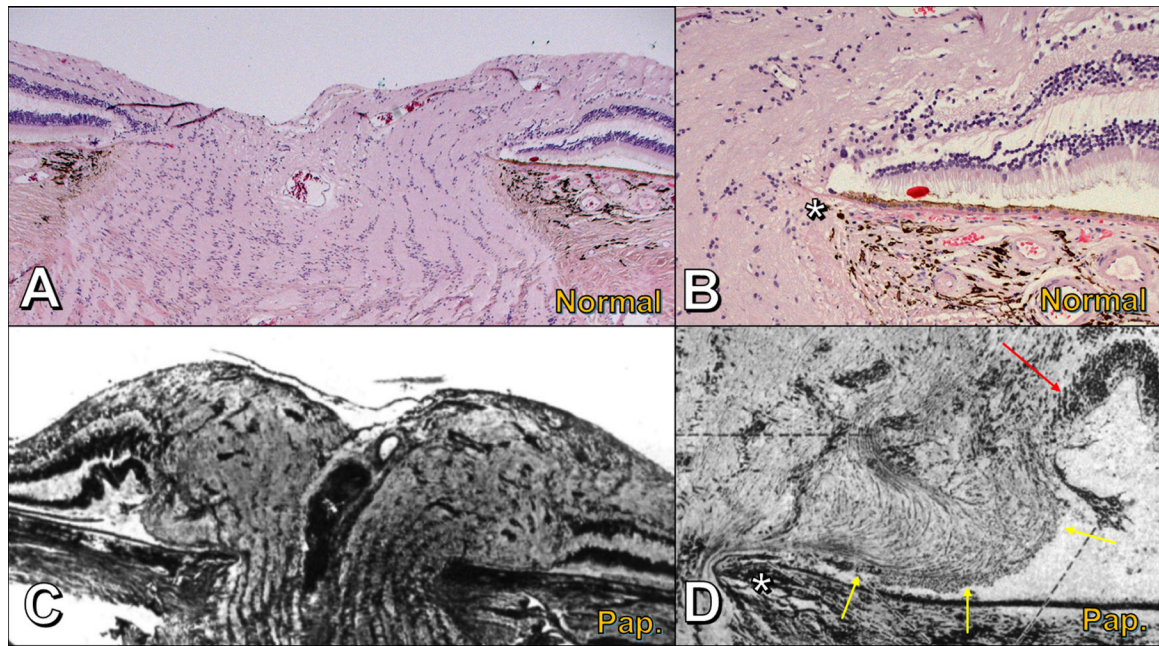
Figure 6 –.

Histomorphology of the optic nerve head; compare normal optic nerve head (A,B) to papilledema (C,D). A) Normal optic nerve head; note the relatively flat, layered architecture of the retinal layers extending right to Bruch's membrane opening (BMO) and narrowing of scleral canal anterior to lamina cribrosa. B) Normal optic nerve head, peripapillary region; optic nerve fibers bend smoothly around Bruch's membrane opening (asterisk) in a gentle C-shaped configuration. C) Papilledema; compared to panel A, the peripapillary retinal layers are displaced laterally (right) or raised and folded (left) by the distended and tortuous prelaminar optic nerve fibers; adapted from (27). D) Papilledema, peripapillary region; compared to panel B, herniating optic nerve fibers above Bruch's membrane opening (asterisk) are bent into an S-shaped configuration; the bottom part of the S forms an ovoid mass-like structure (yellow arrows) that elevates and folds the neighboring retinal layers (red arrow); adapted from (27).
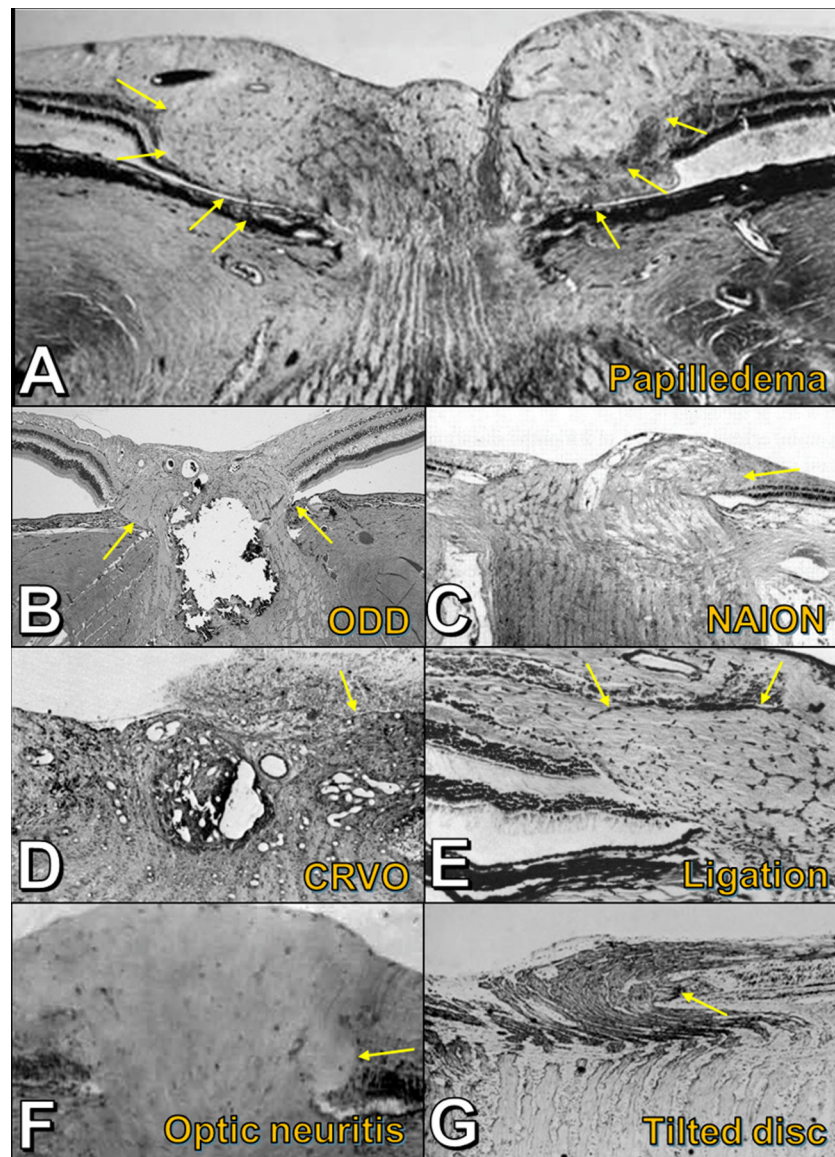
Figure 7 –.
Histopathology in a spectrum of conditions, showing laterally bulging optic nerve fibers (yellow arrows) in response to axoplasmic stasis. A) Papilledema. B) Optic disc drusen. C) Acute nonarteritic anterior ischemic optic neuropathy. D) Acute central retinal vein occlusion. E) Experimental ligation of retrobulbar optic nerve (simian model). F) Acute demyelinating optic neuritis (juvenile guinea pig model). G) Tilted optic disc. Figures adapted with permission as follows: A (44); C (34); D (35); E (36); F (37); G (44).
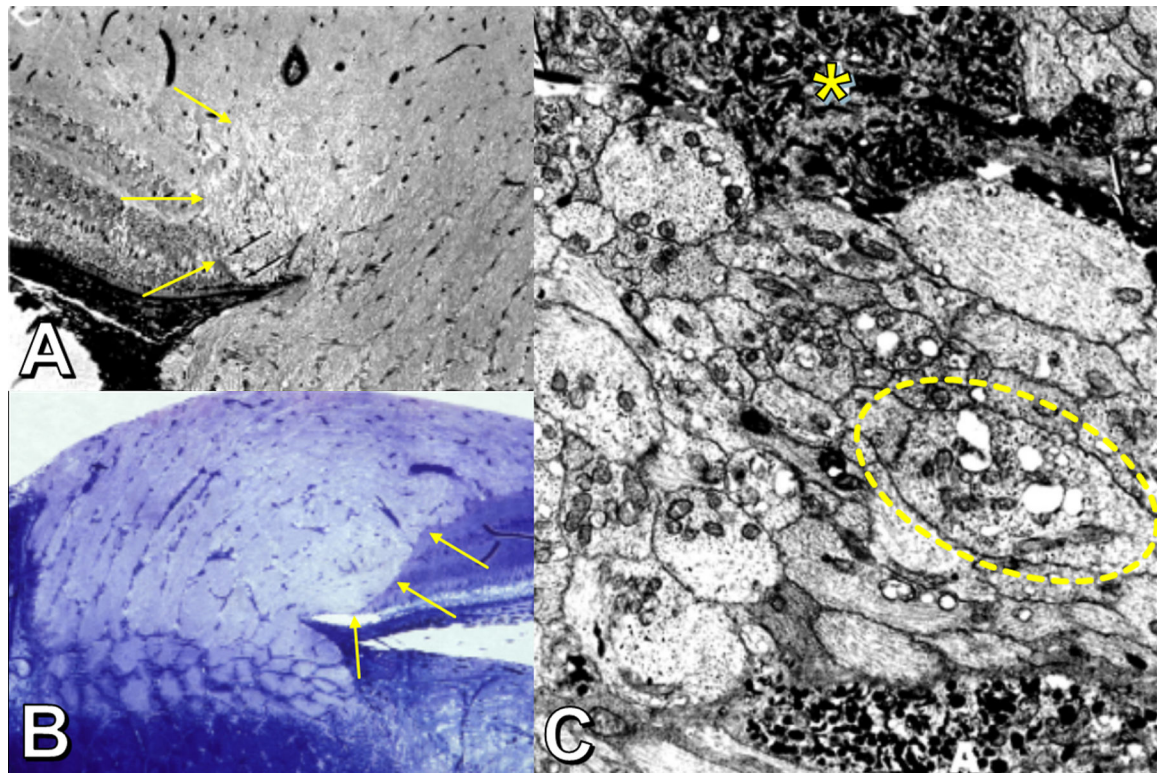
Figure 8 –.
Features of axoplasmic stasis (experimental rhesus model of papilledema). Panels A and B: Histopathology showing lateral bulge of optic nerve fibers (yellow arrows); axons appear vacuolated, abut the retinal pigment epithelium, and displace the retina laterally. Panel C: Electron microscopy showing swollen and vacuolated axons (one shown within dotted oval) with disrupted neurotubules and numerous disorganized mitochondria. The most swollen axons (asterisk) contain large accumulations of giant mitochondria with irregularly arranged cristae and laminated dense bodies (asterisk). Radiotracer studies (not depicted) show obstruction of axonal transport at the level of the lamina cribrosa. Adapted with permission from (26).

Table 1 –

Summary of key differences between PHOMS and ODD

	PHOMS	**ODD**
Location	Strictly peripapillary	Rarely peripapillary; vast majority are found within the optic nerve head (may be superficial or deep)
Histological contents	Distended, vacuolated axons; dilated small venules and capillaries. (In papilledema, interfascicular/intrafascicular edema may also be seen.) Complicated internal substructure with many optical interfaces.	Concentrically-laminated hyaline deposits composed almost entirely of glassy translucent crystalline calcium phosphate. Minimal to no internal substructure. No blood supply.
2D cross-sectional shape	Ovoid, stereotyped; simple with minimal complexity	Sometimes a simple ovoid. Often a lobulated, complex shape or conglomeration of a cluster of ODD.
3D shape	Torus or partial torus; "donut-like"	Ellipsoid; "lump-like"
Reflectivity on EDI-OCT	Uniformly moderately hyperreflective	Brightly hyperreflective outer shell with a darkly hyporeflective core.
OCTA appearance	Dense network of fine blood vessels	No internal microvasculature
Appearance on FAF, US, CT	Undetectable	Detectable – unless deeply buried on FAF, overlooked by US operator, or situated between slices on CT.
Ophthalmoscopic appearance	Hazy peripapillary halo (often C-shaped or O-shaped), most prominent nasally	Glistening refractile lumps within the disc itself
Associated conditions	Papilledema, ODD, NA-AION, CRVO, optic neuritis, tilted optic discs/myopia	Idiopathic, retinitis pigmentosa, pseudoxanthoma elasticum, angioid streaks, Alagille syndrome
Change in appearance over time	Depends on etiology. Can develop *de novo*, fluctuate/regress in concert with degree of disc edema (*e.g.*, papilledema), or may remain static (*e.g.*, tilted optic disc, ODD-associated PHOMS)	No short-term or medium-term change. Never shrink. May grow slowly over decades.

Abbreviations: PHOMS (peripapillary hyperreflective ovoid mass-like structures); ODD (optic disc drusen); EDI-OCT (enhanced-depth imaging optical coherence tomography); US (ultrasound); FAF (fundus autofluorescence imaging); CT (computed tomography); OCTA (optical coherence tomography angiography); NA-AION (nonarteritic anterior ischemic optic neuropathy); CRVO (central retinal vein occlusion).